JACS
JOURNAL OF THE AMERICAN CHEMICAL SOCIETY

Communication

pubs.acs.org/JACS

Toward High Performance *n*-Type Thermoelectric Materials by Rational Modification of BDPPV Backbones

Ke Shi,[†] Fengjiao Zhang,[‡] Chong-An Di,*[,‡] Tian-Wei Yan,[†] Ye Zou,[‡] Xu Zhou,[†] Daoben Zhu,[‡] Jie-Yu Wang,*[,†] and Jian Pei*[,†]

[†]Beijing National Laboratory for Molecular Sciences, Key Laboratory of Bioorganic Chemistry and Molecular Engineering of Ministry of Education, Center for Soft Matter Science and Engineering, College of Chemistry and Molecular Engineering, Peking University, Beijing 100871, China

[‡]Beijing National Laboratory for Molecular Sciences, CAS Key Laboratory of Organic Solids, Institute of Chemistry, Chinese Academy of Sciences, Beijing 100190, China

Supporting Information

ABSTRACT: Three *n*-type polymers **BDPPV**, **ClBDPPV**, and **FBDPPV** which exhibit outstanding electrical conductivities when mixed with an *n*-type dopant, N-DMBI ((4-(1,3-dimethyl-2,3-dihydro-1*H*-benzoimidazol-2-yl)phenyl)dimethylamine), in solution. High electron mobility and an efficient doping process endow **FBDPPV** with the highest electrical conductivities of 14 S cm^{-1} and power factors up to 28 μW m^{-1} K^{-2}, which is the highest thermoelectric (TE) power factor that has been reported for solution processable *n*-type conjugated polymers. Our investigations reveal that introduction of halogen atoms to the polymer backbones has a dramatic influence on not only the electron mobilities but also the doping levels, both of which are critical to the electrical conductivities. This work suggests the significance of rational modification of polymer structures and opens the gate for applying the rapidly developed organic semiconductors with high carrier mobilities to thermoelectric field.

Driven by the prospect of realizing lightweight, low cost, and flexible electricity generation modules, organic materials have attracted increased attention in thermoelectric (TE) research.[1−4] The efficiency of a TE material is determined by the dimensionless figure of merit, $ZT = S^2\sigma T/\kappa$, where S (V K^{-1}) is the Seebeck coefficient or thermopower, σ (S m^{-1}) is electrical conductivity, κ (W m^{-1} K^{-1}) is thermal conductivity, and T is absolute temperature. Generally, as thermal conductivities of organic materials tend to be low (0.1−1 W m^{-1} K^{-1}) and, by contrast, electrical conductivities (10^{-8}−10^4 S cm^{-1}) and Seebeck coefficients (10−10^3 μV K^{-1}) range in a large scale, the TE property can also be evaluated by a parameter called power factor (PF) as $PF = S^2\sigma$ in W m^{-1} K^{-2}. Viable TE devices require both electron and hole conducting materials with high power factors. Although the TE performance of *p*-type organic materials is rapidly advancing,[5−8] there are few examples of high performance *n*-type organic TE materials. Among these materials, vapor-doped fullerenes[9,10] and powder-processed organometallic poly(Ni 1,1,2,2-ethenetetrathiolate) derivatives[11] have demonstrated the highest *n*-type TE performance with electrical conductivities as high as 9 and 40 S cm^{-1} and power factors reaching 30 and 66 μW m^{-1} K^{-2}, respectively. However, these materials are not amenable to solution-processing, severely restricting their extensive application. Recently, several solution-processed *n*-type organic TE materials were reported. Chabinyc demonstrated that solution mixtures of P(NDIOD-T2) with extrinsic dopants, N-DBI derivatives, achieved electrical conductivities of nearly 10^{-2} S cm^{-1} and power factors of up to 0.6 μW m^{-1} K^{-2}.[12] Later, Segalman et al. reported that self-doped perylene diimides exhibited an electrical conductivity of 0.5 S cm^{-1} and power factors of 1.4 μW m^{-1} K^{-2}.[13] Nevertheless, these values are much lower than those obtained for *p*-type TE materials such as PEDOT,[5,6] which necessitates more effort to develop comparable *n*-type TE materials.

As power factor is proportional to electrical conductivity σ, the latter is the product of carrier charge q, carrier concentration n (cm^{-3}), and carrier mobility μ (cm^2 V^{-1} s^{-1}) as $\sigma = nq\mu$. Consequently, high electron mobility and an efficient doping process are prerequisites for high performance *n*-type TE materials. Although organic semiconductors with high electron mobilities have been developing rapidly,[14] efficient and stable *n*-doping is still lagging behind and the relationship between chemical structure and doping level remains unclear.[15−18] In our previous work, we developed a series of **BDPPV** derivatives which exhibited electron mobilities up to 1.70 cm^2 V^{-1} s^{-1} under ambient conditions.[19,20] Besides, the low-lying LUMO levels (below −4.0 eV) make **BDPPV** derivatives the most electron-deficient conjugated polymers reported to date, which is beneficial to an efficient doping process. Herein, we report the electrical conductivities, Seebeck coefficients, and the TE power factors of doped **BDPPV** derivatives and demonstrate that the thin film electrical conductivities could be dramatically enhanced through rational design of molecular structures. To investigate the relationship between chemical structure and the TE property, we develop three **BDPPV** derivatives, **BDPPV**, **ClBDPPV**, and **FBDPPV**, with varied LUMO levels and electron mobilities caused by the halogen atoms. N-DMBI is chosen as the dopant due to its good chemical stability in air and excellent doping ability for a variety of *n*-type semiconductors such as PCBM[16] and P(NDIOD-2T).[12] Through simple structure modification of

Received: January 28, 2015
Published: May 21, 2015

DOI: 10.1021/jacs.5b00945
J. Am. Chem. Soc. 2015, 137, 6979−6982

polymer backbones, we successfully modulate the doping levels to a large degree. Coupled with their excellent electron mobilities, we have achieved electrical conductivities as high as 14 S cm^{-1} and power factors up to 28 $\mu W\ m^{-1}\ K^{-2}$, which leads to the highest TE power factor that has been reported for solution processable *n*-type conjugated polymers.

Figure 1 illustrates the chemical structures of **BDPPV** derivatives and the dopant N-DMBI. **BDPPV**, **ClBDPPV**, **FBDPPV**, and N-DMBI were synthesized and fully characterized (see Supporting Information). All polymers exhibited comparable molecular weights (**BDPPV**: M_n = 41.8 kDa, PDI = 2.39; **ClBDPPV**: M_n = 38.6 kDa, PDI = 2.52; **FBDPPV**: M_n = 42.9 kDa, PDI = 2.36).

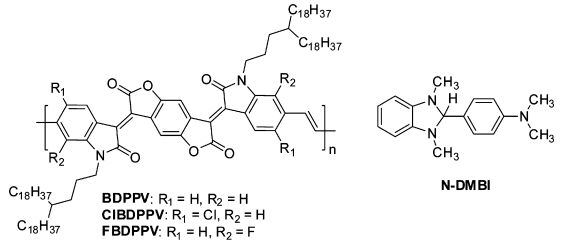

Figure 1. Chemical structures of **BDPPV** derivatives and *n*-type dopant N-DMBI.

The energy levels of **BDPPV** derivatives were explored by cyclic voltammetry to elucidate the effect of halogen atoms (Table S1). After introduction of halogen atoms, both HOMO and LUMO energy levels of **ClBDPPV** and **FBDPPV** are lowered and the LUMO energy levels are more easily affected. The LUMO levels of **ClBDPPV** and **FBDPPV** reach −4.30 and −4.17 eV, 0.29 and 0.16 eV lower than that of **BDPPV**, which make **ClBDPPV** and **FBDPPV** among the most electron-deficient conjugated polymers. Since the LUMOs of all three polymers are higher than the HOMO of N-DMBI (−4.7 eV), a typical hydride transfer reaction between N-DMBI and polymers is operative.[21] As the feasibility of doping is necessarily accompanied by hydride or H atom transfer, the introduction of Cl and F atoms effectively lowers the LUMO levels of polymers and makes **ClBDPPV** and **FBDPPV** stronger C−H bond acceptors. With different reactivity between dopant and polymers induced by halogen atoms, the doping levels of three polymers are likely to be tuned accordingly.

The optical absorption spectrum is usually utilized to indicate the doping process. Therefore, the thin film absorption spectra of three **BDPPV** derivatives with or without doping were characterized. As shown in Figure 2b, all three undoped polymers show similar optical transitions in the visible range due to their identical conjugated backbones and no absorption over 1000 nm was observed. After adding 5 wt % dopant, the dark films dramatically turn light and transparent (Figure 2a). Obviously, there is a considerable amount of neutral units in the films that accepted electrons, leading to the formation of polarons. However, unlike their neutral counterparts, the absorption features of three doped polymers are quite distinct. In Figure 2, a new absorption band around 1100 nm and extending far into the near-infrared region was observed in each doped film, which reasonably originates from polaronic transitions.[5,22,23] Although all three doped films display two major absorption bands (Band I: 1000−1500 nm, Band II: 600−900 nm), but the intensity ratios ($\lambda_{band\ I}/\lambda_{band\ II}$) vary differently. **ClBDPPV** and **FBDPPV** have similar intensity of polaron

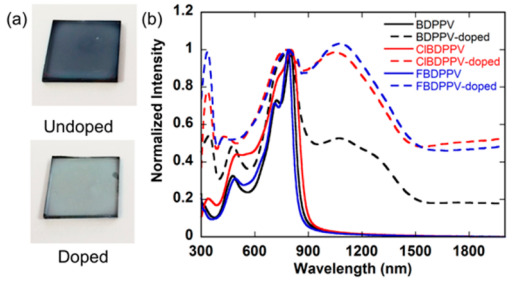

Figure 2. (a) Photographic images of undoped and 5 wt % N-DMBI doped **ClBDPPV** films on glass substrates. (b) Thin film absorption spectra of **BDPPV** derivatives under pristine and doping conditions (5 wt % of N-DMBI) (Normalized at λ_{max} of neutral molecules).

transition, but the one of **BDPPV** is much lower, indicating a lower doping level under the same conditions. The absorption properties show that introduction of halogen atoms to the polymer backbones has remarkable influence on the doping extent.

Further systematic study of doping levels was carried out through XPS characterizations to elucidate the chemical composition in the doped films. As the doping reaction is accompanied by the generation of N-DMBI$^+$,[21] the doping ratios of films could be accurately estimated by analysis of the clearly distinguishable nitrogen peaks N (1s), wherein the amide group of **BDPPV** derivatives (around 400 eV) and the imidazole cation in N-DMBI$^+$ (around 402 eV) were compared. The N (1s) electrons in the imidazole cation have a high binding energy owing to the oxidative quaternary ammonium. Besides, the N (1s) signal of neutral N-DMBI is also at 400 eV, demonstrating that the newly generated N (1s) signal at 402 eV is attributed to the doping reaction. The greater the area of the peak at 402 eV is, the higher the doping level is. As shown in Figure 3, all three

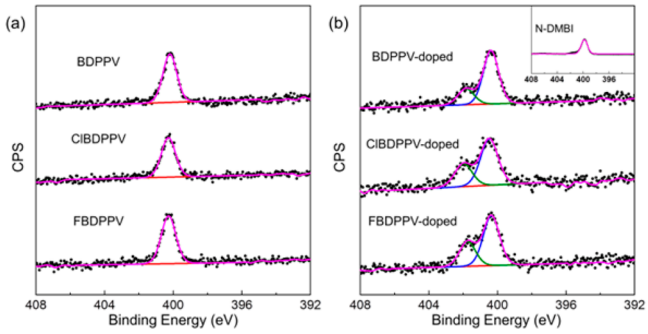

Figure 3. N (1s) XPS spectra of **BDPPV** derivatives (a) in pristine conditions and (b) in doping conditions (5 wt % of N-DMBI). Insert: N (1s) XPS of N-DMBI.

polymers under pristine conditions display the same single peak at 400 eV. After being mixed with N-DMBI, however, the doping ratios among three polymers vary differently. For **BDPPV**, the ratio of peaks at 402 and 400 eV is 25:75, while, for **ClBDPPV** and **FBDPPV**, they are both 33:67. Consequently, the XPS characterization directly confirms that the doping levels of **ClBDPPV** and **FBDPPV** are almost identical and are much higher than that of **BDPPV**, which is in agreement with the result of optical absorption spectra. We further investigated the electronic properties of the undoped and doped films of **BDPPV** derivatives by using ultraviolet photoemission spectroscopy (UPS) (Figure S3). All three doped films exhibited obvious

DOI: 10.1021/jacs.5b00945
J. Am. Chem. Soc. 2015, 137, 6979−6982

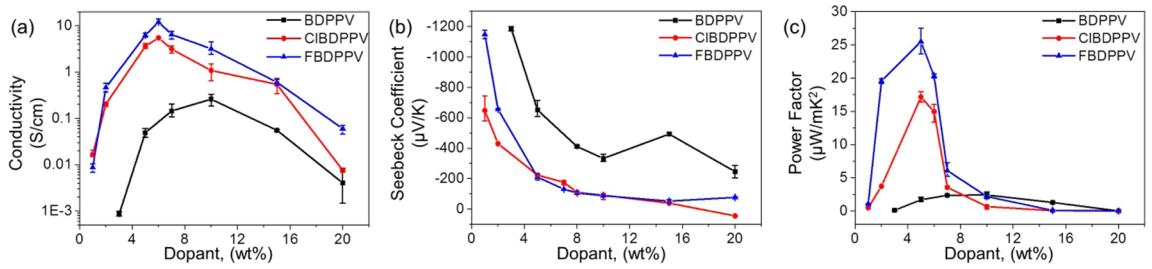

Figure 4. Thermoelectric properties of doped **BDPPV** derivatives at different doping concentrations. (a) Electrical conductivities; (b) Seebeck coefficients; (c) Power factors. Each data point in Figure 4 is an average of at least five devices and showed good repeatability.

shifts of the Fermi level toward higher binding energy, equivalent to an upward movement of E_F toward the LUMO level in band gap, which demonstrates the generation of free electrons and effective *n*-doping.[21]

To characterize the TE properties of **BDPPV** derivatives, the electrical conductivity and Seebeck coefficient were examined. Thin films were prepared from solution mixtures of the polymers and N-DMBI in varied mass fraction by spin-coating on glass substrates with prepatterned gold contacts and thermal annealing at 120 °C for 8 h. Electrical conductivity was measured via a four-probe method, and the Seebeck coefficient was determined by imposing a temperature difference across the sample and measuring the thermovoltages (see Figure S4).

As shown in Figure 4, the electrical conductivities of the films dramatically increase by adding the dopant, and attain maxima as the mass fraction of N-DMBI in solution is 10% for **BDPPV** and 7% for **ClBDPPV** and **FBDPPV**. The Seebeck coefficients of all three polymers are negative, confirming that *n*-type electrical transport is dominant. When the electrical conductivities increase, the Seebeck coefficients change in opposite direction, which is in accord with their negative correlation with carrier concentrations. Further increasing the concentration of N-DMBI leads to a rapid decrease of electrical conductivities and the Seebeck coefficients continue to decline, possibly due to the disruption of polymer morphology or the occurrence of side reactions with excess dopants. Furthermore, Figure 4a reveals that introduction of different halogen atoms to the polymer backbones has a remarkable influence on electrical conductivities. The highest conductivity of **BDPPV** is 0.26 S cm^{-1}, while both **ClBDPPV** and **FBDPPV** show unexpected conductivities over 4 S cm^{-1}, higher by more than an order of magnitude. Moreover, at the optimal doping concentrations (5−10 wt %), the conductivity of **FBDPPV** is roughly twice that of **ClBDPPV**. Notably, the highest conductivity of **FBDPPV** could reach 14 S cm^{-1}. Combination of the electrical conductivity and Seebeck coefficient yields a power factor as high as 28 μW m^{-1} K^{-2} for **FBDPPV** at rt, which is the highest TE performance for solution processable *n*-type polymers. Besides, the dependence of conductivity and the Seebeck coefficient on temperature was investigated. As shown in Figure S5, the conductivity and Seebeck coefficient showed an increasing trend as the temperature increased, which is in accordance with that of typical organic thermoelectric materials reported.[8] The results indicated that the charge transport in these doped polymers can be described by the thermal assisted hopping mechanism.[1] Moreover, all doped polymers exhibited good thermal stabilities in the temperature range of 0−120 °C, and their TE performance also showed good stability for at least 30 days under N_2.

To investigate the effect of dopant amount on surface morphologies, atomic force microscopy (AFM) (Figure S6) was conducted. All undoped thin films display typical fiber-like intercalating networks. Interestingly, after being mixed with 5 wt % dopant, the films of all three polymers display smooth and uniform morphologies with a smaller root-mean-square (rms) roughness of 0.6 nm. Unlike PCBM and P(NDIOD-T2) with high crystallinity,[12,16] thin films of **BDPPV** derivatives doped by N-DMBI present no obvious particles and aggregates on the top of the surface. The low crystallinity of **BDPPV** derivatives ensures better dispersity of dopant in polymer films, thus giving rise to a more efficient doping process. The smooth morphology remains almost unchanged when the dopant concentration increases to 10 wt %. However, when the dopant concentration increases to 20 wt %, both film roughness (over 1.3 nm) and crystalline size of the blend films increase. Overaggregation in the blend films may lower the carrier mobilities, thus leading to the decrease of electrical conductivities. The low crystallinity property of **BDPPV** derivatives is also supported by the grazing incident X-ray diffraction (GIXD) (Figure S7). Three polymers all display weak out-of-plane diffraction peaks along the q_z axis, indicating the relative low crystallinity formed in thin films. After doping with 5 wt % N-DMBI, the weak peaks of polymers essentially remain the same, implying that the ordering of polymers is not likely to be disturbed by the dopant.

To further understand the cause of drops in electrical conductivities, we measured the N (1s) XPS spectra of **BDPPV** derivatives under low (3 wt % of N-DMBI) and high doping conditions (12 wt % of N-DMBI) (Figure S8). From low (3 wt % of N-DMBI) to optimized doping conditions (5 wt % of N-DMBI), the ratios of peaks at 402 and 400 eV had a large increase, which indicated a much higher doping level. The increase of doping levels leads to a higher carrier concentration and enhanced electrical conductivity. However, from optimized (5 wt % of N-DMBI) to high doping conditions (12 wt % of N-DMBI), the ratios of peaks at 402 and 400 eV basically remained constant, which implied no further doping process. In other words, under high doping conditions (12 wt % of N-DMBI), excess N-DMBI did not act as dopants but as impurities and exhibited a negative influence on the polymer packing in thin films. As a consequence, the decrease of electrical conductivities can be attributed to the change of film morphology other than doping levels. Since film morphology has limited influence on Seebeck coefficients, the Seebeck coefficients remained constant as the electrical conductivities started to drop.

As electrical conductivity relies on both charge carrier concentration *n* and carrier mobility μ, we evaluated the electron mobilities to figure out the difference in electrical conductivity among **BDPPV** derivatives. Top-gate/bottom-contact (TG/BC) field-effect transistors were fabricated for both undoped and doped polymers in varied doping concentrations (N-DMBI from 0 to 5 wt %). To ensure the same conditions with electrical

DOI: 10.1021/jacs.5b00945
J. Am. Chem. Soc. 2015, 137, 6979−6982

conductivity characterization, thin films were thermal annealed at 120 °C for 8 h. As shown in Figure S9, all **BDPPV** derivatives based OFET devices exhibited typical *n*-type transporting properties with a large on−off ratio over 10^4 under undoped conditions. When the doping percentage of N-DMBI in thin films increases, the I_{off} (measured at the zero gate voltage) of three polymers increases to different degrees. For **BDPPV**, I_{off} increases from 10^{-9} A to 10^{-4} A in 5 wt % N-DMBI doped devices. However, it is interesting to note that, for **ClBDPPV** and **FBDPPV**, I_{off} has a much larger increase that reaches to over 10^{-3} A with a small on−off ratio (below 2) under the same 5 wt % N-DMBI doped conditions. The huge difference in I_{off} and on−off ratio among the three polymers under same doping concentrations implies different doping levels in the mixed thin films. Further increasing the doping concentrations led to negligible dependence of the $I-V$ characteristic on the gate voltage for all the polymers (Figure S10). In pristine conditions, the electron mobilities of **BDPPV** and **ClBDPPV** are approximately the same with an average mobility of 0.5 $cm^2\ V^{-1}\ s^{-1}$. The mobilities of **FBDPPV**, by contrast, reach an average value of 1.1 $cm^2\ V^{-1}\ s^{-1}$, which is exactly consistent with the difference in electrical conductivities between two polymers. Given the same doping levels of **ClBDPPV** and **FBDPPV** observed from XPS, the difference in their conductivities is very likely attributed to different electron mobilities. The outstanding OFET performance is among the highest values in *n*-type conjugated polymers and is beneficial to achieving high electrical conductivity. Therefore, to obtain high electrical conductivity, both the doping level and the carrier mobility should be taken into account, neither of which is dispensable.

In conclusion, we have developed a series of high performance *n*-type polymers, **BDPPV**, **ClBDPPV**, and **FBDPPV**, for TE applications. All three polymers are capable of effective *n*-type doping after being mixed with dopant N-DMBI in solution. We demonstrate that a record conductivity of 14 S cm^{-1} through a solution doping process can be obtained by rational chemical structure modification. A power factor of 28 $\mu W\ m^{-1}\ K^{-2}$ is also the highest value that has been reported for solution processable *n*-type polymers. Our investigations reveal that introduction of halogen atoms to the polymer backbones has a dramatic influence on not only the electron mobilities but also the doping levels, both of which are critical to the electrical conductivities. Especially, matching of energy levels of polymers and the dopant is a key issue for effective doping. This work opens the gate for applying the rapidly developed organic semiconductors with high carrier mobilities to the thermoelectric field and provides a new viewpoint to investigate the structure−property relationships of doping systems.

■ ASSOCIATED CONTENT

Supporting Information

Experimental details, synthesis, characterization, device fabrication and measurements. The Supporting Information is available free of charge on the ACS Publications website at DOI: 10.1021/jacs.5b00945.

■ AUTHOR INFORMATION

Corresponding Authors

*jieyuwang@pku.edu.cn
*jianpei@pku.edu.cn
*dicha@iccas.ac.cn

Notes

The authors declare no competing financial interest.

■ ACKNOWLEDGMENTS

This work was supported by the Major State Basic Research Development Program (Nos. 2013CB933501 and 2015CB856505) from the Ministry of Science and Technology, National Natural Science Foundation of China and Beijing Natural Science Foundation (2144049). The authors thank Prof. Ya-Pei Wang, Xin-Yue Zhang from Renmin University of China and Dr. Deng-Li Qiu from Bruker AXS GmbH Beijing Representative Office for AFM measurements. The authors thank beamline BL14B1 (Shanghai Synchrotron Radiation Facility) for providing the beam time.

■ REFERENCES

(1) Bubnova, O.; Crispin, X. *Energy Environ. Sci.* **2012**, *5*, 9345.
(2) McGrail, B. T.; Sehirlioglu, A.; Pentzer, E. *Angew. Chem., Int. Ed.* **2015**, *54*, 1710.
(3) Poehler, T. O.; Katz, H. E. *Energy Environ. Sci.* **2012**, *5*, 8110.
(4) Zhang, Q.; Sun, Y.; Xu, W.; Zhu, D. *Adv. Mater.* **2014**, *26*, 6829.
(5) Bubnova, O.; Khan, Z. U.; Malti, A.; Braun, S.; Fahlman, M.; Berggren, M.; Crispin, X. *Nat. Mater.* **2011**, *10*, 429.
(6) Kim, G. H.; Shao, L.; Zhang, K.; Pipe, K. P. *Nat. Mater.* **2013**, *12*, 719.
(7) Bubnova, O.; Berggren, M.; Crispin, X. *J. Am. Chem. Soc.* **2012**, *134*, 16456.
(8) Zhang, Q.; Sun, Y.; Xu, W.; Zhu, D. *Energy Environ. Sci.* **2012**, *5*, 9639.
(9) Menke, T.; Ray, D.; Meiss, J.; Leo, K.; Riede, M. *Appl. Phys. Lett.* **2012**, *100*, 093304.
(10) Sumino, M.; Harada, K.; Ikeda, M.; Tanaka, S.; Miyazaki, K.; Adachi, C. *Appl. Phys. Lett.* **2011**, *99*, 093308.
(11) Sun, Y.; Sheng, P.; Di, C.; Jiao, F.; Xu, W.; Qiu, D.; Zhu, D. *Adv. Mater.* **2012**, *24*, 932.
(12) Schlitz, R. A.; Brunetti, F. G.; Glaudell, A. M.; Miller, P. L.; Brady, M. A.; Takacs, C. J.; Hawker, C. J.; Chabinyc, M. L. *Adv. Mater.* **2014**, *26*, 2825.
(13) Russ, B.; Robb, M. J.; Brunetti, F. G.; Miller, P. L.; Perry, E. E.; Patel, S. N.; Ho, V.; Chang, W. B.; Urban, J. J.; Chabinyc, M. L.; Hawker, C. J.; Segalman, R. A. *Adv. Mater.* **2014**, *26*, 3473.
(14) Zhao, Y.; Guo, Y.; Liu, Y. *Adv. Mater.* **2013**, *25*, 5372.
(15) Naab, B. D.; Zhang, S.; Vandewal, K.; Salleo, A.; Barlow, S.; Marder, S. R.; Bao, Z. *Adv. Mater.* **2014**, *26*, 4268.
(16) Wei, P.; Oh, J. H.; Dong, G.; Bao, Z. *J. Am. Chem. Soc.* **2010**, *132*, 8852.
(17) Li, C.-Z.; Chueh, C.-C.; Ding, F.; Yip, H.-L.; Liang, P.-W.; Li, X.; Jen, A. K. Y. *Adv. Mater.* **2013**, *25*, 4425.
(18) Walzer, K.; Maennig, B.; Pfeiffer, M.; Leo, K. *Chem. Rev.* **2007**, *107*, 1233.
(19) Lei, T.; Xia, X.; Wang, J.-Y.; Liu, C.-J.; Pei, J. *J. Am. Chem. Soc.* **2014**, *136*, 2135.
(20) Lei, T.; Dou, J.-H.; Cao, X.-Y.; Wang, J.-Y.; Pei, J. *J. Am. Chem. Soc.* **2013**, *135*, 12168.
(21) Naab, B. D.; Guo, S.; Olthof, S.; Evans, E. G. B.; Wei, P.; Millhauser, G. L.; Kahn, A.; Barlow, S.; Marder, S. R.; Bao, Z. *J. Am. Chem. Soc.* **2013**, *135*, 15018.
(22) Mai, C.-K.; Schlitz, R. A.; Su, G. M.; Spitzer, D.; Wang, X.; Fronk, S. L.; Cahill, D. G.; Chabinyc, M. L.; Bazan, G. C. *J. Am. Chem. Soc.* **2014**, *136*, 13478.
(23) Beaujuge, P. M.; Vasilyeva, S. V.; Ellinger, S.; McCarley, T. D.; Reynolds, J. R. *Macromolecules* **2009**, *42*, 3694.

DOI: 10.1021/jacs.5b00945
J. Am. Chem. Soc. 2015, 137, 6979−6982